Modulation of stimulated emission of ZnO nanowire based on electromechanical vibration

LIJIE LI[1*]

[1]*College of Engineering, Swansea University Bay Campus, Fabian Way, Swansea SA1 8EN, UK*
**Corresponding author: lijie.li@hotmail.co.uk*

Abstract: An optical modulator is proposed using the double clamped nanoelectromechanical resonator. Electro-mechanical-optical analysis has been performed to validate the idea. The electromechanical simulation involves the nonlocal effect as the resonator is in nanometre scale. Stimulated emission theory has been used to model the luminescence of the nanowire due to the addition of piezoelectric charges subjecting to mechanical strains. Results successfully demonstrate both the intensity modulation and frequency filtering, providing an integrated solution in applications such as quantum entanglement experiments.

OCIS codes: *(130.4110) Modulators, (130.3990) Micro-optical devices, (160.4236) Nanomaterials.*

1. INTRODUCTION

Recent advances in nanotechnology have greatly promoted research and development of many engineering and science areas. A variety of nanomaterials have emerged attracting vast interests form international researchers. In particular one of the nanomaterials (ZnO) has been extensively researched, which includes ZnO thin films used in sensors [1], ZnO nanowires used in energy harvesting [2], electronics [3], and sensors [4]. The most attractiveness of this material is the co-existence of semiconducting and piezoelectric properties [5], which can be utilized to construct devices whose performances are adjustable by the piezoelectric effect. Inspired by the phenomenon of the mechanical pressure induced change of the optical emission in the ZnO nanowires [6], it is reasonable to propose a device that can modulate the incident light using a nanoelectromechanical systems (NEMS) resonator made of piezoelectric materials such as ZnO. The nanometre resonator based optical modulator will have all the advantages of the ordinary MEMS/NEMS resonators such as very high frequency dynamic behaviour [7], which can be applied as an electronic device for radio communications [8], high sensitivity mass sensors [9], nanoscale mass spectrometers [10], label-free detection of specific biological molecules and cells [11]. Due to the optical modulation behaviour, the deflection of the resonator can be read through output optical spectrum in the case of device being applied as sensors. The device can be also employed as an adjustable optical modulator. In recent century, quantum internet has been intensively investigated, which requires transmitting quantum states encoded into photons between nodes of the networks[12]. In the experimental setup for quantum entanglements, intensity modulation is heavily needed[13] [14], which is currently accomplished by acousto-optic modulator (AOM). In this work, a high frequency Electro-mechanical optic modulation has been introduced using the resonating nanowire, which possesses both intensity modulation and frequency filtering functions. Multiphysical simulation has been conducted to validate this idea. The paper starts from electromechanical analysis of the ZnO nanowire resonator to find out its dynamic behaviour, followed by quantum optics analysis of the stimulated emission from the nanowire. Through combined opto-electro-mechanical analysis, the demonstration of optical modulation mechanism is presented.

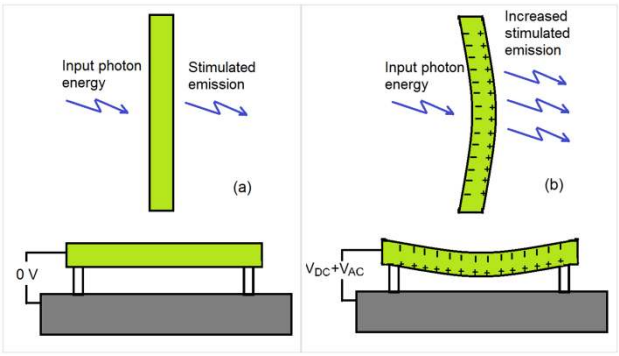

Fig. 1. Schematic of the optical modulation. The amplitude of stimulated emission of the nanowire can be tuned by increasing the number of the free electrons, and the piezoelectric mechanism is used to increase the number of the free electrons. The modulation of the light can be achieved using deformed piezoelectric nanowire. (a) The nanowire is at original position. (b) The nanowire is deformed by external electrostatic force, and extra electron-hole pairs created by piezoelectric effect enhance the stimulated emission.

2. ELECTRO-MECHANICAL MODEL

The vibrating mechanical device in the design can be structured by a double clamped nanowire resonator driven by the electrostatic force applied between itself and the bottom electrode (Figure 1). Normally the driving voltage $V(t)$ is the combination of ac and dc components, expressed by V_{DC} and $V_{AC}\cos(\omega_f t)$, respectively, where ω_f is the driving frequency. The cylindrical nanowire has length L and diameter r. The material of the nanowire is chosen to be ZnO having density ρ, Young's modulus Y and moment of inertia I. Because of the nanometer scale of the resonator, mechanical nonlocal effect is considered in calculating the dynamic behaviour [15]. The nonlocal stress tensor $\vec{\sigma}_N$ is expressed by:

$$\vec{\sigma}_N = \int_{\Omega} N\left(\left|\vec{x}' - \vec{x}\right|, v\right)\vec{\sigma}(\vec{x}')d\vec{x}' \qquad (1)$$

where $N\left(\left|\vec{x}' - \vec{x}\right|, v\right)$ is the nonlocal modulus in which $\left|\vec{x}' - \vec{x}\right|$ is the distance between two points in the lattice. $\vec{\sigma}(\vec{x}')$ is the stress tensor without considering the nonlocal effect. v is the material-depended parameter. In order to consider the nonlocal theory into the beam dynamic equation, the Eq. (1) can be equivalently expressed as [16] [15]:

$$\left(1 - u_0^2\nabla^2\right)\vec{\sigma}_N = \vec{\sigma}, \quad u_0 = v^2L_{in}^2 = p_0^2L_{ex}^2 \qquad (2)$$

where L_{in} and L_{ex} are the internal and external characteristic lengths, p_0 is the material constant. By combining the nonlocal theory and beam dynamic theory, the equation describing the motion of the nanowire resonator can be written as [17]:

$$\begin{aligned}&\rho A_a(\ddot{W} - u_0\ddot{W}'') + d_r(\dot{W} - u_0\dot{W}'') - \rho I(\ddot{W} - u_0\ddot{W}'')'' \\ &+ YIW'''' - (T_{in} + T_i)(W - u_0W'')'' = F - u_0F''\end{aligned} \qquad (3)$$

where $W(x,t)$ is the dynamical displacement of the resonator along the x-axis, with the dot and prime denoting the differentiation with respect to the t and x, respectively. T_i and T_{in} are the initial and induced mechanical tension in the nanowire, respectively. A_s is the cross-section of the nanowire. $F(x,t)$ and d_r are the distributed force applied on the nanowire and the damping ratio, respectively, and they have been derived in previous work [18] , as:

$$\begin{aligned}F &= -\frac{\pi\varepsilon_a V^2(t)}{(Z+d)[\ln(4\frac{W(x,t)+d}{r})]^2} \qquad (4)\\ &\approx -\frac{2\pi\varepsilon_a(V_{DC}V_{AC})\cos(\omega_f t)}{h[\ln\frac{4d}{r}]^2} = F_0\cos(\omega_f t)\end{aligned}$$

$$d_r = -\frac{\pi Pd}{4v_T} \qquad (5)$$

where ε_a is the dielectric constant of the gaseous medium surrounding the resonator. d is the initial distance between the nanowire and the bottom electrode. In Eq. (4), the approximation has been made based on the assumption that the displacement of the nanowire is much smaller than the gap d. P and T_k are the air pressure and temperature respectively, $v_T = \sqrt{k_BT_k/m_a}$ is the air molecule velocity at T_k, and k_B is the Boltzmann constant. m_a is molecular mass of air. Galerkin's method has been employed [16] [19] in order to calculate the deflection of the centre of the nanowire, by which $W(x,t)$ can be written as: $W(x,t) = z(t)\Phi(x)$, where $\Phi(x) = (2/3)^{1/2}[1-\cos(2\pi x/L)]$ is the deflection eigenmode and $z(t)$ is the time dependent displacement of the nanowire centre. $\Phi(x)$ has the boundary conditions: $\varphi(0) = \varphi(L) = \varphi''(0) = \varphi''(L) = 0$. Substituting $W(x,t) = z(t)\Phi(x)$ into Eq. (3) and multiplying $\Phi(x)$ on both sides of the equation, then integrating the equation from 0 to L, the equation for the centre displacement z of the nanowire is:

$$\begin{aligned}&\left(\rho A_a\left(L + u_0\frac{4\pi^2}{3L}\right) + \rho I\left(\frac{4\pi^2(L^2+4u_0\pi^2)}{3L^3}\right)\right)\ddot{z} \\ &+ d_r\left(L + u_0\frac{4\pi^2}{3L}\right)\dot{z} + \left(YI\left(\frac{16\pi^4}{3L^3}\right) + T_i\left(\frac{4\pi^2(L^2+4u_0\pi^2)}{3L^3}\right)\right)z \\ &+ \frac{YA_a}{2L}\left(\frac{16\pi^4(L^2+4u_0\pi^2)}{9L^4}\right)z^3 = -2\frac{\pi\varepsilon_a V_{dc}V_{ac}}{h(\ln(4h/d))^2}\left(\sqrt{\frac{2}{3}}L\right)\cos(\omega_f t)\end{aligned} \qquad (6)$$

Numerical simulation can be conducted to arrive at the dynamic displacement of the nanowire centre, from which the curvature of the deflected nanowire is calculated. In the fundamental mode, the deflected nanowire can be considered as a partial arc, whose curvature C_k is reciprocal of the total radius R_t, expressed as

$$C_k = \frac{1}{R_t} = 1/\left(\frac{z}{2} + \frac{L^2}{8z}\right) \qquad (7)$$

According to piezoelectric theory, due to the stress and strain of the vibrating clamped-clamped beam, electrical charge can be generated if the nanowire is made of a piezoelectric material. Coupling of the stress T_s and strain S, electrical field E_e and electrical displacement D is explained by

$$\begin{aligned}S &= s_{11}^E T_s + d_{31}E_e \\ D &= d_{31}T_s + \varepsilon_{31}^T E_e\end{aligned} \qquad (8)$$

where d_{31} and ε_{33}^T are the transverse coefficient and permittivity of the piezoelectric material at constant stress, respectively. s_{11}^E is the mechanical compliance. The strain S of the surface of the nanowire can be described in terms of the curvature C_k

$$S = C_k z_s \qquad (9)$$

where z_s is the distance from the neutral plane. For the circular cross-section of the nanowire, the neutral plane is the horizontal line across the origin. A quarter of the circle is divided to N sections, and the distance between each section and the neutral line is $z_s(i) = \frac{r}{2}\sin(\frac{\pi i}{2N})$, $i = 1,2,3,\ldots N$. Neglecting the external electrical field E_e = 0, the stress distributed in the piezoelectric beam is given by

$$T_s = \frac{S}{s_{11}^E} = \frac{1}{s_{11}^E}C_k z_s = YC_k z_s \qquad (10)$$

Then the electrical charge generated on the top half of the surface by the stress within the piezoelectric nanowire is

$$\begin{aligned}Q &= \frac{\pi Lr^2 d_{31}Y}{4}C_k\sum_{i=0}^{N}\frac{1}{N}\sin\left(\frac{\pi i}{2N}\right) \qquad (11)\\ &= \frac{2z\pi r^2 Ld_{31}Y}{\left(4z^2+L^2\right)}\sum_{i=0}^{N}\frac{1}{N}\sin\left(\frac{\pi i}{2N}\right)\end{aligned}$$

In equation (5), d_r is the damping ratio that is determined by the quality of the surrounding air $d_r = -\frac{\pi Pd}{4v_T}$ $v_T = \sqrt{k_BT_k/m_a}$, where P and T_k are the air pressure and temperature respectively, v_T is the air molecule velocity at T_k, k_B is the Boltzmann constant and m_a is molecular mass of air. In the initial calculation, we set T_k =300 K, P=1.01325x10^5 Pa, and m_a=5.6x10^{-26} kg, resulting in a d_r=5.85x10^{-6}. If the surrounding

pressure is changed to a smaller values, i.e. *P* is within the range of 0.05x10^5 Pa – 1x10^5 Pa), comparison of the maximum displacement for the driving condition of V_{dc}=0.5 V and V_{ac}=1 V has been made as shown in Figure 2a. It is shown that the temperature of the surrounding air makes difference and the relationship of the temperature vs. maximum displacement is also displayed in the Figure 2b.

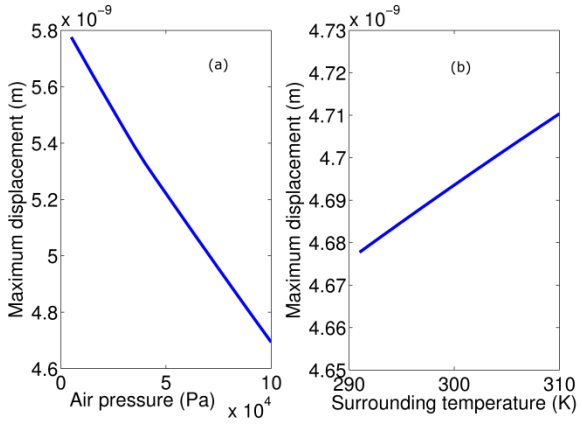

Fig. 2. Calculated impact due to surrounding air properties (pressure (a) and temperature (b)) on the dynamic displacement of the electrostatic actuated double clamped nanowire.

3. SIMULATION OF OPTICS

Next we will theoretically validate the hypothesis that varying charge density of the material modulates the stimulated emission by the quantum optics theory, more specifically Fermi golden rule describing light-matter interactions. It is supposed that the incident light is expressed by an electromagnetic wave express as $A(r,t) = A_0 \cos(q \cdot r - \omega t)$, where the wave vector $q = \frac{\omega n_r}{c}$, n_r is the refractive index of the media, *c* is the speed of incident light and ω denotes the angular frequency of the plane wave. The stimulated emission rate caused by an electron migrating from high energy states to low energy states is described by the golden rule, which is

$$R = \frac{2\pi}{\hbar}\left|\langle \psi_2 | H' | \psi_1 \rangle\right|^2 \delta(E_c - E_v - \hbar\omega) \qquad (12)$$

where ψ_1 and ψ_2 are the initial and final states respectively, *H'* is the perturbation Hamiltonian $H' = \frac{e}{2m} A_0 e^{iq\cdot r} \cdot q$ caused by the incident wave. $\hbar$ is the reduced Planck's constant. E_v and E_c are conduction band minimum and valence band maximum respectively. Indicated in the equation (12), the transition rate *R* is determined by the strength of the coupling between initial and final states. Assume that a number of transitions happening per unit volume *V* of material per second, the total transition rate is the sum of the all transition probabilities, that is

$$R_{St} = \frac{2}{V}\left(\sum_k R\right) f_e f_h \qquad (13)$$

where f_e and f_h are Fermi-Dirac distribution functions of electrons and holes in the material respectively ($\frac{1}{e^{(E-\mu)/k_BT}+1}$). Mathematic derivations on the equations (12) & (13) can arrive at the expression of the sum of the transitions per unit volume as

$$\frac{2}{V}\sum_k R = \frac{2\pi}{\hbar}\left(\frac{qA_0}{2m}\right)^2 \left\langle \left|\hat{\vec{p}}\cdot\hat{\vec{n}}\right|^2 \right\rangle \times 2\int \frac{d^3k}{(2\pi)^3}\delta(E_c - E_v - \hbar\omega) \qquad (14)$$

where $\left|\hat{\vec{p}}\cdot\hat{\vec{n}}\right|^2$ is squared momentum matrix element depending on the electron wave vector *k* and also the polarization direction of the incident electromagnetic wave. In most of III-V and II-IV semiconductors, a constant value of the matrix can be given to the average value $\left\langle \left|\hat{\vec{p}}\cdot\hat{\vec{n}}\right|^2 \right\rangle$ of the momentum matrix element [20], expressed in terms of the Kane energy E_k, as $\left\langle \left|\hat{\vec{p}}\cdot\hat{\vec{n}}\right|^2 \right\rangle = \frac{mE_k}{6}$. The value of E_k for some of semiconductor materials can be found from [21] [22]. The 3D integral $\int \frac{d^3k}{(2\pi)^3}\delta(E_c - E_v - \hbar\omega)$ is the density of states (DOS), *g(E)* in three-dimensions. Bandgap $E_g = E_c - E_v$. *g(E)* is defined as the number of states in a conductor per unit energy. For nanostructures, electrons are likely confined in three dimensions, like quantum dots. The DOS for electrons confined in 3D is

$$g(E) = \frac{2}{\pi}\frac{\hbar/2\tau}{(\hbar\omega - E_g)^2 + (\hbar/2\tau)^2} \qquad (15)$$

The width of the Lorentzian (equation (15)) at half its peak value (full width at half maximum, or FWHM) is $\hbar/\tau$. The coupling between the photon and the electron within the nanowire can be described by the coupling energy $\Gamma = \hbar/\tau$. In this work, the Γ is taken to be 20 meV. Substitute equation (15) to equation (14), one can get

$$R_{st} = \frac{2\pi}{\hbar}\left(\frac{qA_0}{2m}\right)^2 \left\langle \left|\hat{\vec{p}}\cdot\hat{\vec{n}}\right|^2 \right\rangle \times \frac{2}{\pi}\frac{\Gamma/2}{(\hbar\omega - E_g)^2 + (\Gamma/2)^2} f_e f_h \qquad (16)$$

Re-arrange equations (7), let $M = \left\langle \left|\hat{\vec{p}}\cdot\hat{\vec{n}}\right|^2 \right\rangle$, and substitute *q* by $(\omega n_r)/c$, it becomes

$$E_{st} = \frac{4A_0^2 M}{m^2\hbar^3 c^2}(\hbar\omega)^2 n_r^2 \frac{\Gamma/2}{(\hbar\omega - E_g)^2 + (\Gamma/2)^2} f_e f_h \qquad (17)$$

where $\hbar\omega$ is the photon energy. It is seen that the stimulated emission is determined by the combined effect from the incident photon energy, refractive index, DOS and Fermi distributions of electrons and holes. According to equation (17), stimulated emissions have been calculated numerically. The chemical potential for a number of electrons and holes per unit volume at certain temperatures is required to calculate the f_e and f_h. To calculate the chemical potential for electrons or holes, the following process is used. First of all, an initial value of the chemical potential needs to be estimated. The maximum possible value of the chemical potential is given by the Fermi energy $\mu_{\max} = E_F = \frac{\hbar^2 k_F^2}{2m}$ $k_F = (3\pi^2 n_c)^{1/3}$, n_c is the carrier density. The minimum possible value of the chemical potential is given by the high-temperature limit ($T \to \infty$). In this limit the Fermi-Dirac distribution becomes Boltzmann distribution

$$f(E)\big|_{T\to\infty} = \frac{1}{e^{(E-\mu)/k_BT}+1}\Big|_{T\to\infty} = e^{(E-\mu)/k_BT} \qquad (18)$$

A three dimensional electron gas in this high temperature limit has chemical potential

$$\mu_{\min} = k_B T \ln\left(\frac{n}{2}\left(\frac{2\pi\hbar^2}{mk_B T}\right)^{3/2}\right) \qquad \textbf{(19)}$$

Carrier density n' can be calculated using an integral over energy

$$n' = \frac{1}{2\pi^2}\left(\frac{2m}{\hbar^2}\right)^{3/2}\int_{E_{\min}=0}^{E_{\max}=\infty} E^{1/2}\frac{1}{e^{(E-\mu)/k_B T}+1}dE \qquad \textbf{(20)}$$

A computer iteration process is used to calculate the chemical potential for both electrons and holes respectively (μ_e, μ_h). In the process, an initial chemical potential value taking the average of the maximum and minimum chemical potential is used to calculate a carrier density n' for a given temperature by calculating the integral described by the equation (20). If the n' is less than the actual value n_c, the new best estimate for $\mu_{\min} = \mu'$. The new estimated μ is given, and the process iterate until the value reaches to a desired level of accuracy. The calculated chemical potentials for electrons and holes are then used in equation (17) to calculate the stimulated emission rate.

Numerical calculation is conducted to demonstrate the modulation effect through jointly solving equations (6), (11), and (17). In the calculations, the nanowire has the length and diameter of 3 μm and 20 nm. Young's modulus and density of ZnO are taken as 240 GPa and 5610 kg/m^3. Distance between nanowire and the bottom electrode is assumed as 200 nm. Standard parameters for the Planck's and Boltzmann constants are used. Nonlocal factor of 0.04*L^2 is designated in the mechanical simulation. Bandgap of 3.375 eV is used for the ZnO nanowire. Firstly, low driving voltages (V_{dc} = 0.5 V, V_{ac} = 1 V) are applied, under which the results are shown in Figure 3.

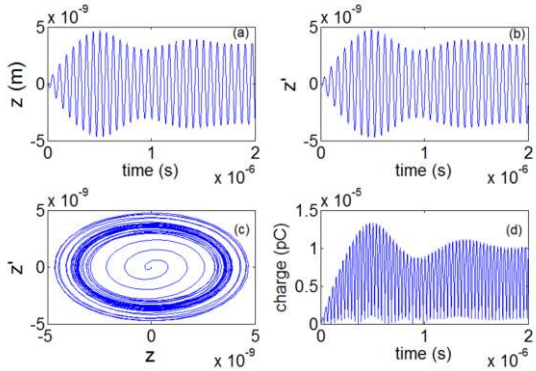

Fig. 3. Simulation results of the vibrating nanowire from the starting time to stabilized periodic vibration. The driving condition is V_{dc} = 0.5 V, V_{ac} = 1 V. (a) Displacement versus time. (b) Velocity versus time. (c) Phase space trajectory shows the vibration is periodic. (d) Charge generation versus time.

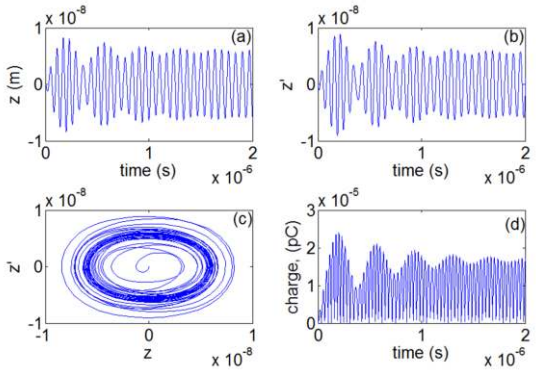

Fig. 4. Dynamic behaviour of the optical modulator under V_{dc} = 1 V, V_{ac} = 2 V. (a) Displacement versus time. (b) Velocity versus time. (c) Phase space of the system indicates it is still in periodic state. (d) Charge induction over time.

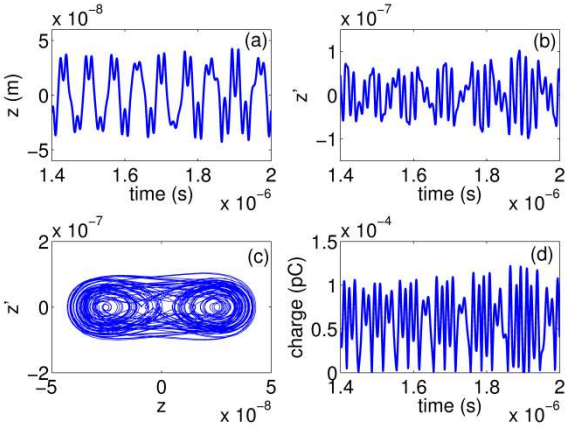

Fig. 5. Dynamic behaviour under large driving signals, V_{dc} = 15 V, V_{ac} = 20 V. (a) Displacement versus time. (b) Velocity graph. (c) Trajectory demonstrates chaotic vibration. (d) Charge generation in correlation with the vibration amplitude.

Figures 3-5 are results from dynamic theory described by the differential equation 6 together with the piezoelectric charge generation theory by the equation 11. Figure 6 has been obtained from the combination of dynamic theory and stimulated emission theory described in the equation 17. The vertical axis in Figure 6 is calculated emission amplitude from the equation 17. The values of intensity have a relative unit (a.u.) to show scaled intensity expression $\frac{E_{SI} m^2 \hbar^3 c^2}{4A_0^2 M}$. Filter effect (resonances in Fig. 7a) due to mechanical strains can be demonstrated with ZnO materials. In the calculation, the wavelength of the stimulating light varies from 360 nm to 380 nm, there is a calculated peak emission at wavelength of 367 nm (Fig. 7a). The relationship between wavelength of the light and the stimulated emission is governed by the Fermi Golden rule (Equations 12 and 17). Experimentally this resonance effect (filtering effect) was observed in reference [23].

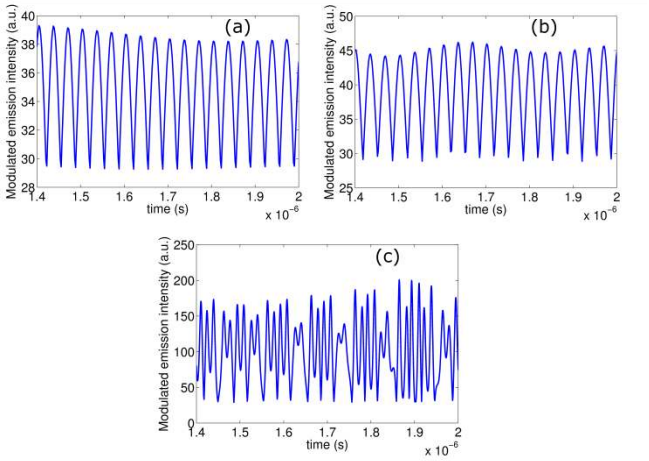

Fig. 6. Modulated peak amplitude of the optical emission. (a) Periodic modulation stabilized at 94.2 MHz. (b) Periodic modulation for slightly larger amplitude, same resonant frequency as in (a). (c) Chaotic modulation at large driving signals.

Figures 3a-3c display results for the deformation, velocity and trajectory, all of which prove that under such driving conditions, the nanowire oscillates periodically. This is attributed to that under small signal driving conditions; the oscillating amplitude is small, therefore the z^3 term in the equation 6 is much smaller than the linear term z. Hence the dynamic vibration of the nanowire is dominated by the linear term. Figure 3d displays generated charges corresponding dynamic strains in Figure 3a. The results in Figure 3d are obtained by the combined electro-mechanical-piezo-optical procedure. Essentially large displacement induces more free piezoelectric charges, subsequently generating much more stimulated emissions. Increasing driving voltages to (V_{dc} = 1 V, V_{ac} = 2 V), changes on the deformation and velocity are observed together with related piezoelectric charges, which are shown in Figures 4a-4d, where the nanowire resonator still vibrates at the periodic manner. It is expected that nonlinear behavior will appear when the driving voltages are extraordinary large. This is proven by using (V_{dc} = 15 V, V_{ac} = 20 V), the results shown in Figures 5a-5d clearly demonstrate that the device is at the chaotic state. Modulated emission intensities under the above three driving conditions have been simulated using the Golden rule and results are displayed in Figure 6. It indicates that modulation effect can be achieved by the piezoelectric nanowire, which may find promising applications in nanometer sized optical laser sources, high sensitivity sensors. Static simulation on the stimulated emissions using various carrier densities from small to large, corresponding to small to large deflections has been performed, which is displayed in Figure 7. Figure 7a shows the increasing emission intensity for large carrier density and demonstration of the filtering effect, and Figure 7b shows scaled emissions (from dim to bright) of three wires undergoing small to large deflections. In Figure 7a, the Δn represents strain induced piezoelectric charges. Increasing piezoelectric charges will affect the Fermi-distributions fe and fh through equations 18-20. More piezoelectric charges will increase stimulated emission according to the equation 17. For stimulated emission, the emitted light has the same wavelength as the excitation light, hence it is used to increase the amplitude of the stimulating light for the purpose of making lasing [24]. In the calculation, the wavelength of the stimulating light varies from 360 nm to 380 nm, there is a calculated peak emission at wavelength of 367 nm (Fig. 7a). The relationship between wavelength of the light and the stimulated emission is governed by the Fermi Golden rule (Equations 12 and 17). The proposed idea is to use electrostatic force to deflect the nanowire, therefore generating electrons based on piezoelectric effect. These generated electrons will then increase the amplitude of the stimulated emission. Amplitude modulation is achieved by applying electrostatic force on the piezoelectric nanowire. The radiation pressure (PR) of the incident light can be used to generate strain of mechanical structures. However the RP force is usually very small, and these mechanical strains are only about a few Å [25] [26], which is not enough to induce any piezoelectric charges. To summarise, the main theories used here are piezoelectric induced charges (equation 11) and Fermi golden rule (equation 17). For the equation 11, it has been mainly derived from the classic piezoelectric constitutive equation (equation 8) following the procedure described in [27]. With regards to the equation 17, it is from the Fermi Golden rule that is widely used for describing stimulated emission rate.

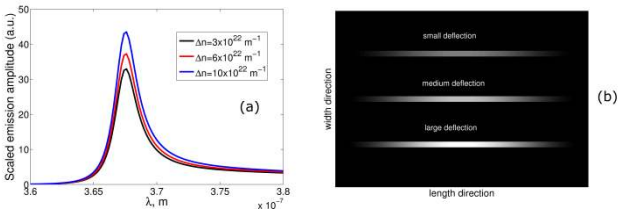

Fig. 7. Optical emission when the nanowire experiences static deformation. (a) Stimulated emission spectrum at different induced charges. (b) Simulated emission of the double clamped nanowire for different deflection amplitudes.

4. CONCLUSION

In summary, a new optical modulator is reported using a double clamped vibrational nanowire. The wire is made of piezoelectric material; so that the vibration induced charge generation modulates the stimulated emission intensity. In this way an electrical controllable optical modulator can be achieved. Coupled electro-mechanical-optical model has been constructed and subsequently simulated. Results demonstrate intensity modulations of the optical signal through driving the nanowire in periodic and non-periodic oscillations. Nanoelectromechanical resonator normally having fast response speed will have great potential in atomic-physics and spectroscopic applications.

Acknowledgment. The author is grateful for support from the college of engineering, Swansea University.

References

1. P. Mitra, A. P. Chatterjee, and H. S. Maiti, "ZnO thin film sensor," Materials Letters 35, 33-38 (1998).
2. B. Kumar and S.-W. Kim, "Energy harvesting based on semiconducting piezoelectric ZnO nanostructures," Nano Energy 1, 342-355 (2012).
3. L. Li, "Electromechanical resistive switching via back-to-back Schottky junctions," AIP Advances 5, 097138 (2015).
4. R. Yu, C. Pan, and Z. L. Wang, "High performance of ZnO nanowire protein sensors enhanced by the piezotronic effect," Energy & Environmental Science 6, 494-499 (2013).
5. Z. Wang, "Basic Theory of Piezotronics," in *Piezotronics and Piezo-Phototronics* (Springer Berlin Heidelberg, 2012), pp. 51-72.
6. C. Pan, L. Dong, G. Zhu, S. Niu, R. Yu, Q. Yang, Y. Liu, and Z. L. Wang, "High-resolution electroluminescent imaging of pressure distribution using a piezoelectric nanowire LED array," Nat Photon 7, 752-758 (2013).
7. K. Eom, H. S. Park, D. S. Yoon, and T. Kwon, "Nanomechanical resonators and their applications in biological/chemical detection: Nanomechanics principles," Physics Reports 503, 115-163 (2011).

8. P. X. L. Feng, "Nanoelectromechanical systems: Tuning in to a graphene oscillator," Nat Nano 8, 897-898 (2013).
9. K. L. Ekinci, X. M. H. Huang, and M. L. Roukes, "Ultrasensitive nanoelectromechanical mass detection," Applied Physics Letters 84, 4469-4471 (2004).
10. P. A. Greaney and J. C. Grossman, "Nanomechanical Resonance Spectroscopy: A Novel Route to Ultrasensitive Label-Free Detection," Nano Letters 8, 2648-2652 (2008).
11. A. P. Davila, J. Jang, A. K. Gupta, T. Walter, A. Aronson, and R. Bashir, "Microresonator mass sensors for detection of Bacillus anthracis Sterne spores in air and water," Biosensors and Bioelectronics 22, 3028-3035 (2007).
12. H. J. Kimble, "The quantum internet," Nature 453, 1023-1030 (2008).
13. E. Togan, Y. Chu, A. S. Trifonov, L. Jiang, J. Maze, L. Childress, M. V. G. Dutt, A. S. Sorensen, P. R. Hemmer, A. S. Zibrov, and M. D. Lukin, "Quantum entanglement between an optical photon and a solid-state spin qubit," Nature 466, 730-734 (2010).
14. E. Saglamyurek, J. Jin, V. B. Verma, M. D. Shaw, F. Marsili, S. W. Nam, D. Oblak, and W. Tittel, "Quantum storage of entangled telecom-wavelength photons in an erbium-doped optical fibre," Nat Photon 9, 83-87 (2015).
15. A. C. Eringen, "On differential equations of nonlocal elasticity and solutions of screw dislocation and surface waves," Journal of Applied Physics 54, 4703-4710 (1983).
16. A. C. Eringen, "Nonlocal polar elastic continua," International Journal of Engineering Science 10, 1-16 (1972).
17. F. Najar, S. El-Borgi, J. N. Reddy, and K. Mrabet, "Nonlinear nonlocal analysis of electrostatic nanoactuators," Composite Structures 120, 117-128 (2015).
18. Q. Chen, L. Huang, Y.-C. Lai, C. Grebogi, and D. Dietz, "Extensively Chaotic Motion in Electrostatically Driven Nanowires and Applications," Nano Letters 10, 406-413 (2010).
19. J. Gao, J. M. Luther, O. E. Semonin, R. J. Ellingson, A. J. Nozik, and M. C. Beard, "Quantum Dot Size Dependent J–V Characteristics in Heterojunction ZnO/PbS Quantum Dot Solar Cells," Nano Letters 11, 1002-1008 (2011).
20. G. Jacopin, L. Rigutti, A. Bugallo, F. Julien, C. Baratto, E. Comini, M. Ferroni, and M. Tchernycheva, "High degree of polarization of the near-band-edge photoluminescence in ZnO nanowires," Nanoscale Research Letters 6, 501 (2011).
21. V. A. Fonoberov and A. A. Balandin, "ZnO quantum dots: Physical properties and optoelectronic applications," Journal of Nanoelectronics and Optoelectronics 1, 19-38 (2006).
22. P. Lawaetz, "VALENCE-BAND PARAMETERS IN CUBIC SEMICONDUCTORS," Physical Review B 4, 3460-& (1971).
23. X. Fu, Z.-M. Liao, R. Liu, F. Lin, J. Xu, R. Zhu, W. Zhong, Y. Liu, W. Guo, and D. Yu, "Strain Loading Mode Dependent Bandgap Deformation Potential in ZnO Micro/Nanowires," ACS Nano 9, 11960-11967 (2015).
24. S. C. Singh, H. Zeng, C. Guo, and W. Cai, "Lasers: Fundamentals, Types, and Operations," in *Nanomaterials* (Wiley-VCH Verlag GmbH & Co. KGaA, 2012), pp. 1-34.
25. T. Carmon, H. Rokhsari, L. Yang, T. J. Kippenberg, and K. J. Vahala, "Temporal Behavior of Radiation-Pressure-Induced Vibrations of an Optical Microcavity Phonon Mode," Physical Review Letters 94, 223902 (2005).
26. L. Jin and L. Li, "Optical driven electromechanical transistor based on tunneling effect," Optics Letters 40, 1798-1801 (2015).
27. L. Jin, J. Mei, and L. Li, "Analysis of intrinsic localised mode for a new energy harvesting cantilever array," The European Physical Journal - Applied Physics 66, 10902 (2014).